Biophysical Chemistry 159 (2011) 33–40

Contents lists available at ScienceDirect

Biophysical Chemistry

journal homepage: http://www.elsevier.com/locate/biophyschem

Stability, denaturation and refolding of *Mycobacterium tuberculosis* MfpA, a DNA mimicking protein that confers antibiotic resistance

Sergei Khrapunov *, Michael Brenowitz *

Department of Biochemistry, Albert Einstein College of Medicine, 1300 Morris Park Avenue, Bronx, NY 10461, USA

ARTICLE INFO

Article history:
Received 31 March 2011
Received in revised form 25 April 2011
Accepted 25 April 2011
Available online 5 May 2011

Keywords:
Pentapeptide repeat protein
CD
Fluorescence
Protein folding
MfpA
Antibiotic resistance

ABSTRACT

MfpA from *Mycobacterium tuberculosis* is a founding member of the pentapeptide repeat class of proteins (PRP) that is believed to confer bacterial resistance to the drug fluoroquinolone by mimicking the size, shape and surface charge of duplex DNA. We show that phenylalanine side chain stacking stabilizes the N-terminus of MfpA's pentapeptide thus extending the DNA mimicry analogy. The Lumry–Eyring model was applied to multiple spectral measures of MfpA denaturation revealing that the MfpA dimer dissociates to monomers which undergo a structural transition that leads to aggregation. MfpA retains high secondary and tertiary structure content under denaturing conditions. Dimerization stabilizes MfpA's pentapeptide repeat fold. The high Arrhenius activation energy of the barrier to aggregate formation rationalizes its stability. The mechanism of MfpA denaturation and refolding is a 'double funnel' energy landscape where the 'native' and 'aggregate' funnels are separated by the high barrier that is not overcome during *in vitro* refolding.

1. Introduction

The *Mycobacterium tuberculosis* protein MfpA is a founding member of the pentapeptide repeat class of proteins (PRP). MfpA confers resistance to the antibiotic fluoroquinolone. Recent studies have shown that the size, shape, and electrostatic surface potential of MfpA are sufficiently similar to B-form DNA to suggest that these properties mimic those of DNA [1,2]. Competition for DNA binding via mimicry is proposed to explain inhibition of DNA gyrase activity by MfpA with the resultant resistance to the antibiotic fluoroquinolone [3–5].

MfpA has the propensity to denature *in vitro* into a nonnative structure that irreversibly aggregates upon denaturation [6]. Irreversible protein denaturation and the formation of aggregates is not just an *in vitro* artifact; it has been implicated in human pathology [7] and can complicate bacterial over expression of proteins [8]. Unlike the well-developed thermodynamic theory of the reversible denaturation and refolding proteins [9,10], a general theory describing irreversible folding has not been developed. Clearly, the character of protein denaturation and refolding reactions depends on the structure and stability of the intermediates formed. Long-range ordering can precede formation of a native protein conformation under highly denaturing conditions [11] or in the 'molten globule' state [12,13]. Residual secondary and/or tertiary structure in denatured protein can create structural nuclei promoting formation both native and non-native monomeric or oligomeric structures.

The novelty of the PRP fold has motivated our investigations into the structure and stability of MfpA and its irreversible denaturation reaction. In addition, the conjecture that MfpA mimics a deformed rather than straight DNA duplex when binding to DNA gyrase [4] suggests that the structure and/or the dynamics of the N-terminus of the protein that include the dimerization interface may play a unique functional role. In the present paper we explore the relationships between MfpA stability, dimerization and the propensity of the denatured protein to aggregate.

2. Materials and methods

2.1. Protein and buffer preparation

The expression and purification of *M. tuberculosis* MfpA in *Escherichia coli* is described elsewhere [1,6]. All experiments were conducted at pH 7.6 and 22.0 °C (except for the temperature induced transitions). Temperature induced denaturation was conducted in buffer containing 10 mM KH_2PO_4, 25 mM KCl and 2 mM DTT. Sodium dodecyl sulfate (SDS) induced denaturation was conducted in 5 mM Tris–HCl, 5 mM KCl and 2 mM DTT. Urea induced denaturation was conducted in 25 mM Tris–HCl, 25 mM KCl, 4 mM $MgCl_2$, 0.1 mM EDTA, 6% Glycerol and 2 mM DTT. Since the MfpA stock solution contains glycerol and NaCl and most experimental samples were prepared by dilution, trace amounts of those components are present in the experimental samples. Control experiments were conducted to confirm that identical MfpA fluorescence and CD spectral parameters were observed in all of the buffers. MfpA concentration was determined by absorption using $\varepsilon_{280} = 17{,}070\ M^{-1} \times cm^{-1}$ (MfpA monomer).

* Corresponding authors. Tel.: +1 718 430 3180; fax: +1 718 430 8565.
E-mail addresses: khraps@einstein.yu.edu (S. Khrapunov), michael.brenowitz@einstein.yu.edu (M. Brenowitz).

0301-4622/$ – see front matter © 2011 Elsevier B.V. All rights reserved.
doi:10.1016/j.bpc.2011.04.015

2.2. Circular dichroism (CD) spectroscopy

Far-UV CD spectra were recorded in either a 1 or 2 mm quartz cuvette on a J-810 spectropolarimeter (Jasco Inc., Easton, MD) equipped with a PTC-423S Peltier temperature control unit. Scans of 1–4 μM solutions of MfpA were recorded from 240 to 190 nm at a band width of 1 nm and scanning speed of 50 nm/min. Three spectral accumulations were averaged. Near-UV CD spectra were recorded from 320 to 260 nm as described above. The MfpA concentrations are reported in the figure legends. The buffer contribution was subtracted from CD spectra expressed as the molar ellipticity, [θ], in deg·cm^2·dmol^{-1}. Background was not subtracted from CD spectra expressed as a relative change in ellipticity (θ in millidegrees).

2.3. Fluorescence and light scattering spectroscopy

Fluorescence measurements were made using a Fluoromax-3 spectrofluorometer (Jobin Yvon Inc., USA). Intrinsic fluorescence spectra were obtained by excitation at 280 nm with the emission monitored from 300 to 450 nm. The spectra are routinely corrected for the spectral sensitivity of the instrument. Measurements were made at the *magic angle* of 55° between the excitation and emission polarization vectors. The buffer contribution was subtracted in all of the experiments. The intensity of the Raman scattering band of water is the internal standard of spectrofluorometer sensitivity. Fluorescence anisotropy was calculated by

$$A\lambda = \frac{Iv - GIh}{Iv + 2GIh} \tag{1}$$

where $A\lambda$ is the fluorescence anisotropy measured at a combination of the excitation and emission wavelengths with the excitation polarizer in the vertical position, *Iv* and *Ih* are the fluorescence intensities measured at the vertical and horizontal position of the emission polarizer, and *G* is the instrumental factor accounting for the bias of the detection system for vertically versus horizontally polarized light.

The ratio $^{F1}/_{F2}$ is a sensitive parameter reflecting a shift of fluorescence λ_{max} with an accuracy not less than ± 0.2 nm [14] where F1 and F2 are the fluorescence intensities at the half-width of fluorescence spectra obtained at an experimental condition. Elastic Light Scattering (ELS) was also recorded using the Fluoromax-3 spectrofluorometer. Scattered light (350 nm) was collected at an angle of 90° to the incident light.

2.4. MfpA denaturation and refolding by temperature

CD and fluorescence **t**hermal stability experiments were performed in buffer (section 2.1) between 10 and 90 °C with a constant heating rate of 1 °C/min. The Lumry–Erying model of protein denaturation [15] that invokes a rate limiting stage leading to an irreversible structural transition of the protein was used to fit the experimental temperature denaturation data of MfpA. We derived a convenient expression for calculation of the integral of the Arrhenius function based on the asymptotic expansion of the rational approximations (see Supplement). This expression can be applied to any biologically relevant process with an accuracy of 1.7 to 0.07% for a value of Ea/RT between 10 and 50. The equation

$$f_N = \exp\left(-{}^{1}\!/_{v}\, \exp({}^{a}\!/_{Tk})\frac{T^2}{a(\exp(a/T)}\right) \tag{2}$$

was derived from this expression where f_N is the molar fraction of native state, $v = dT/dt$ is the scanning rate, $a = E_a/R$ where E_a is the Arrhenius activation energy and *R* is the gas constant and *Tk* is the temperature at which the first-order rate constant given by the Arrhenius equation, $k = 1\ min^{-1}$, The denaturation transitions were fit to Eq. (2) using Origin v6.1 (MicroCal). The basis for applying the Lumry–Eyring model to this analysis and the development of Eq. (2) are described in the Supplement.

The melting temperature was determined by fitting to transitions to

$$f_N = \frac{1}{1 + \exp\left(\left(T - T_{1/2}\right)/sT\right)} \tag{3}$$

where f_N is the molar fraction of native state, *T* is the temperature, $T_{1/2}$ is the mid-point of the transition and *sT* is the slope of the transition at $T_{1/2}$. Analysis using Eqs. (2) and (3) assumes that the pre- and post-denaturation base lines are linear and can be extrapolated into the transition. Accordingly, $f_N = (Y_{obs} - Y_D)/(Y_N - Y_D)$, where Y_{obs} is the measured parameter. $Y_N = k1^*x + Y_{N0}$ and $Y_D = k2^*x + Y_{D0}$ where Y_N and Y_D are the pre- and post-transition base lines, *k*1 and *k*2 are the fitted parameters and Y_{N0} and Y_{D0} are initial and final values of the measured parameters at $T = 0$ K. The assumption of linear base lines is supported by the fluorescence change that occurs upon denaturation [16] and by the slight perturbation in the pre- and post-transition regions (Fig. 2) that is consistent with temperature-dependent changes in protein fluorescence [17].

2.5. MfpA denaturation and refolding by urea

Aliquots of MfpA to be analyzed spectrally were dissolved in buffer containing 10 mM KH_2PO_4, 25 mM KCl and 2 mM DTT without or with 6.5 M urea and then passed into solution containing indicated concentration of urea. Sample solutions were incubated at the experimental temperature for 24 h prior to taking measurements. The MfpA concentrations are provided in the legends to the figures.

2.6. MfpA denaturation and refolding by SDS

Aliquots from 2.0 and 100.0 mM SDS stock solutions prepared in buffer containing 5 mM Tris–HCl, 5 mM KCl and 2 mM DTT were added stepwise to the protein dissolved in the same buffer. The samples were incubated 3 h at the experimental temperature before measurements were taken. Time course measurements demonstrated that this incubation time is sufficient to reach equilibrium (data are not shown). MfpA denaturation titrations as a function of SDS concentration were fit to

$$Yobs = Yo + (Y\ max - Yo)^*\left({}^{x^n}\!/_{(k_d + x^n)}\right) \tag{4}$$

where *Yobs*; *Ymax* and *Yo* represent the observed, infinite and initial values of the measured parameter, *n* is the number of binding sites occupied by SDS per MfpA monomer, *x* is the unbound concentration of SDS and k_d is the apparent dissociation constant [18].

2.7. Ultracentrifugation

High speed centrifugation was performed using a TLA-120.2 rotor in a Beckman Optima TLX ultracentrifuge at 80,000 rpm and 4 °C for 15 min.

3. Results

3.1. Thermal denaturation and refolding of MfpA

Temperature-induced denaturation and refolding of MfpA was monitored by CD to follow changes in backbone conformation, intrinsic fluorescence to follow oligomerization changes and exposure of the core of the PRP fold and light scattering to follow aggregation. The characteristic far UV CD spectrum of dimeric MfpA [6] is evident at 20 °C with negative peaks at 195 and 218 nm (Fig. 1A, solid line). As the temperature

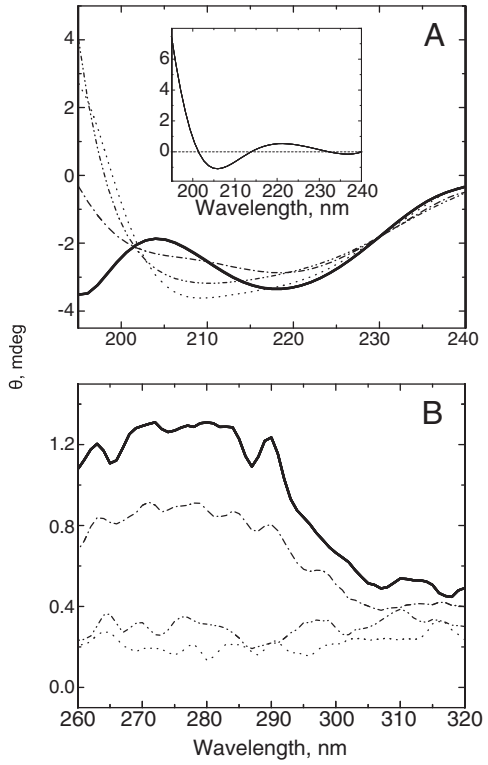

Fig. 1. The (A) far-UV (2 μM) and (B) near-UV CD-spectra (17.7 μM) of MfpA as a function of temperature in buffer containing 10 mM potassium phosphate, 25 mM KCl, 2 mM DTT at pH 7.6 (20 °C, solid line; 55 °C, dash-dotted line; 90 °C, dash-double dotted line; and refolded to 20 °C following cooling from 90 °C, dotted line). Inset (A): the difference spectra far-UV CD spectra between 90 and 20 °C.

is increased, the 195 nm negative peak becomes positive, the 218 nm peak smoothes and a new peak at 208 nm appears. The native structure vanishes by 70 °C after which the spectrum is unchanged up to 90 °C, the highest temperature analyzed (Fig. 1A, dashed line). The CD spectrum at 90 °C does not resemble a denatured protein but rather that of α/β proteins [19]. The difference far-UV CD spectrum calculated between 90 and 20 °C shows two bands at 195 and 205 nm (Fig. 1A, *inset*); the temperature-dependent transition followed using the 205 nm band is highly concerted (Fig. 2A; Table 1).

Coupled oscillator interactions between aromatic side chains are the source of the signal for the near-UV CD spectrum of MfpA. The coupled oscillator interactions are distance dependent with shorter distances normally leading to a stronger CD signal [20,21]. Although the wavelength assignment of aromatic CD bands is not precise, the assigned ranges [22] indicate that phenylalanine is the greatest contributor to the MfpA near-UV CD spectrum with the 290 nm peak reflecting tryptophan.

Together the high temperature CD spectra indicate a highly structured protein lacking the ordering around the aromatic residues characteristic of native MfpA. The presence of appreciable structure at high temperature is corroborated by MfpA's tryptophan fluorescence; the high temperature emission λ_{max} is intermediate to the emission λ_{max} values characteristic of native and denatured by urea proteins, respectively (332<340<356 nm; Fig. 3A).

While fluorescence intensity and quantum yield are directly related to the mole fraction of states of the protein, emission λ_{max} and anisotropy are not [16]. However, the ratio F1/F2 (done at the half-width for convenience; Fig. 2B, inset) is a state function since it normalizes for quantum yield differences as λ_{max} changes [14]. Temperature-induced denaturation of MfpA monitored by F1/F2 is highly concerted with a lower T_m and higher activation energy than that deduced from the CD transitions (Fig. 2B; Table 1).

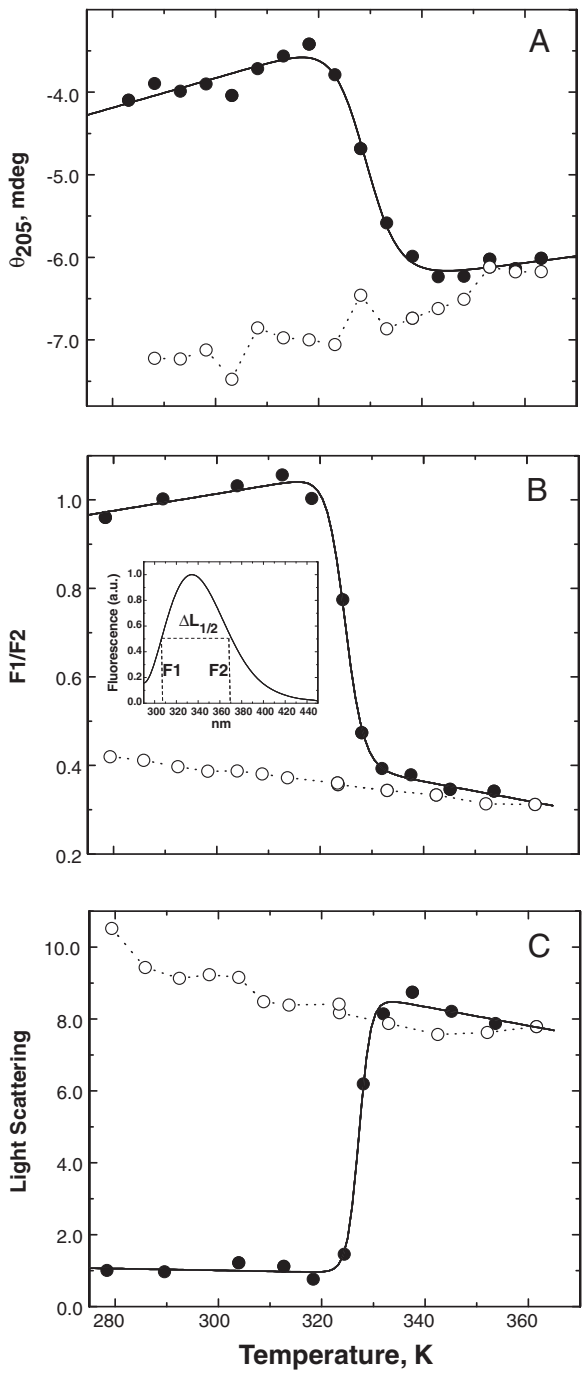

Fig. 2. Temperature induced denaturation and aggregation of 2 μM MfpA in buffer containing 10 mM potassium phosphate, 25 mM KCl, 2 mM DTT at pH 7.6. The solid circles denote temperature dependent denaturation. The open circles denote refolding from 90 °C. A) The change in ellipticity at 205 nm ($T_{1/2}=55.4\pm0.4$ °C). B) The change of the ratio of fluorescence at wavelengths on the wings of spectrum (F1/F2; insert) following excitation at 280 nm ($T_{1/2}=51.3\pm0.3$ °C). Inset: The fluorescence spectrum of MfpA illustrating the half-width of the spectrum ($\Delta\lambda_{1/2}$) and the calculation of the ratio, F1/F2. C) The change of light scattering measured at an angle of 90° to the incident illumination ($T_{1/2}=54.0\pm0.2$ °C).

MfpA aggregation during denaturation was followed by Elastic Light Scattering (ELS). The ELS signal increases ten-fold as the temperature is elevated (Fig. 2C). The ELS, CD and fluorescence intensity transitions have identical values of T_m within experimental error (Fig. 2, Table 1; Supplementary Fig. 1S). We fit these transitions to the Lumry–Eyring model that describes this irreversible reaction as a two step kinetic model N↔I→F. Since the rate-limiting step is

Table 1
Energetic parameters characterizing the temperature dependent unfolding of *M. tuberculosis* MfpA.

Method[d]	E_a (kcal/mol)[a]	T_k (°C)[b]	T_m (°C)[c]
CD_{205}	44.8 ± 4.0	65.3 ± 1.3	55.4 ± 0.4
F1/F2	69.5 ± 6.9	55.9 ± 0.7	51.3 ± 0.3
ELS	161.1 ± 35.6	55.0 ± 0.4	54.0 ± 0.2
F_{int}	65.6 ± 5.7	60.6 ± 0.8	55.1 ± 0.3

[a] E_a, Arrhenius activation energy.
[b] T_k, temperature at which k (the first-order rate constant given by the Arrhenius equation) equals one (min^{-1}).
[c] T_m – melting temperature.
[d] CD_{205}, ellipticity at 205 nm; F1/F2, the ratio of the fluorescence intensities at the wings of the fluorescence spectrum; ELS, Elastic Light Scattering; F_{int}, integral fluorescence intensity.

denaturation, the formation of F can be approximated as N → F. (See the supplement for the complete derivation.) This analysis provides the Arrhenius activation energy reported by each spectral measure (Table 1). The ELS transition is very steep resulting in a greater Arrhenius activation energy than that calculated from the other spectral measures. Since aggregation is a concentration dependent process, it does not occur before the concentration of the transformed MfpA molecules (as reported by CD and fluorescence) is sufficient to initiate aggregation. The high Arrhenius aggregation activation energy that is calculated for aggregation rationalizes the stability of the aggregate and its inability to dissociate upon cooling.

We next sought to partition the CD, F1/F2 fluorescence ratio and ELS transitions (Figs. 1 & 2) into the relative changes in MfpA secondary, tertiary and quaternary structure. Our goal is to determine whether the changes in these components are independent, sequential or connected. The two additional fluorescence measures that aid this analysis are the fluorescence spectrum half-width ($\Delta\lambda_{½}$; defined in Fig. 2B, insert) and F_{int}, the integral fluorescence intensity (Supplementary Fig. 1S). F_{int} is a direct measure of the fraction of the different MfpA conformers in solution; its sharp transition at $T_m = 55.1 \pm 0.3$ °C is almost coincident with the secondary structure change reported by CD ($T_m = 55.4 \pm 0.4$ °C).

Since the fluorescence emission spectrum of the protein is a sum of the spectra of its fluorophores (three tryptophan residues in this case), $\Delta\lambda_{½}$ is a *qualitative* parameter that reflects changes in microenvironment surrounding the fluorophores. We observe that $\Delta\lambda_{½}$ becomes smaller at high temperatures. This decrease reflects greater homogeneity in the environment surrounding the tryptophan residues of MfpA within the non-native aggregate compared with native MfpA. The $\Delta\lambda_{½}$ transition tracks with the other spectral signals (Supplementary Fig. 1SB). The F1/F2 transition at lower temperature ($T_m = 51.3 \pm 0.3$ °C) reflects dissociation of the MfpA dimer into monomers which subsequently undergo a structural transition monitored by the other spectral parameters (Table 1).

In summary, these data show that the changes in MfpA secondary, tertiary and quaternary structure do *not* occur coincidently during temperature dependent denaturation. Rather, MfpA dimers first dissociate into monomers. Under the denaturing condition of elevated temperature the monomers undergo a structural transition that predisposes them to aggregation. In order to characterize the denaturation intermediates we extended our analysis to include chemical and detergent mediated denaturation.

3.2. Urea denaturation and refolding of MfpA

MfpA denaturation, refolding and aggregation were also studied using the chemical denaturant urea. The fluorescence spectra obtained for native, urea denatured and refolded from urea MfpA have distinct fluorescence intensity and emission λ_{max} values (Fig. 3A). Urea addition red shifts λ_{max} from ~332 to 356 nm. Urea denaturation isotherms were generated for the fluorescence intensity ratio F1/F2, ELS (Fig. 4A & B) and fluorescence anisotropy (Supplementary Fig. 2S). The fluorescence data together reflect an increase in the polarity and mobility of the tryptophan residues. The ELS denaturation transition differs from the fluorescence titrations by peaking at 2.5–3.0 M urea, midway through the fluorescence transition, and then decreasing to the original level (Fig. 4B). The irreversibility of urea denaturation described below precludes calculation of thermodynamic parameters by linear extrapolation [23,24].

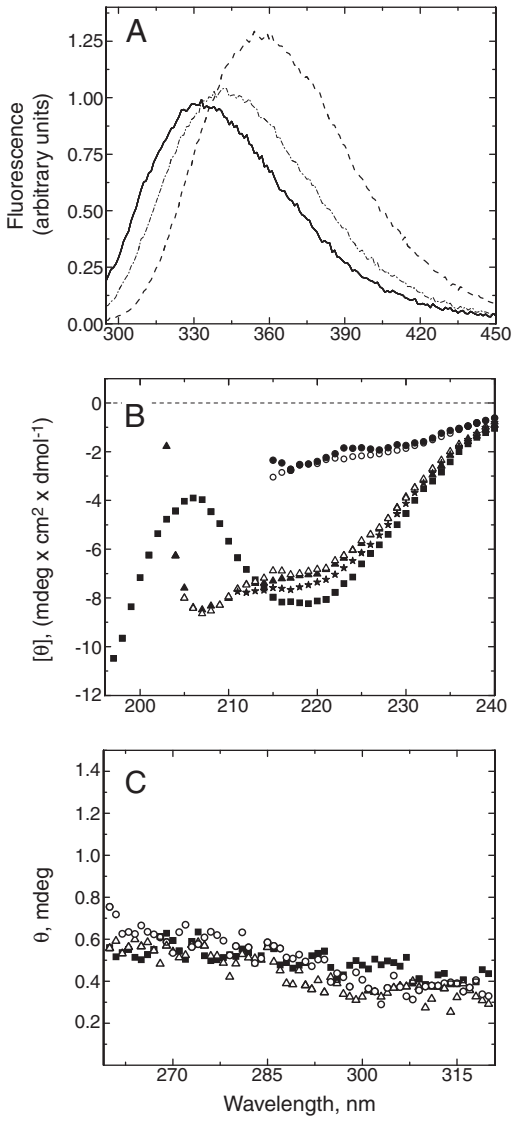

Fig. 3. A) The fluorescence emission spectra measured upon excitation at 280 nm of native (solid line), denatured (dashed line) and refolded from 6.5 M urea (dot-dashed line) MfpA. The protein concentration is 1 μM; B) The far-UV CD-spectra of MfpA at different concentrations in buffer (squares, open & filled triangles and stars) and 6.5 M urea (open and filled circles). The concentrations of MfpA are 4 μM – native (filled squares), denatured (filled circles), refolded (filled triangles); 7 μM – refolded (open triangles); 11 μM – denatured (open circles); 21.3 μM – refolded (stars). **C)** The near-UV CD-spectra of buffer (filled squares), denatured MfpA (11 μM, in 6.5 M urea, open triangles) and refolded MfpA (21.3 μM, buffer, open circles). The buffer is 10 mM potassium phosphate, 25 mM KCl, 2 mM DTT at pH 7.6.

Refolding by either dialysis or dilution results in a partial blue shift of the fluorescence spectrum to $\lambda_{max} \approx 342$ nm. The far-UV CD spectrum of MfpA refolded from urea is characterized by the 206 nm peak observed for the temperature refolded protein (Figs. 1A & 3B). This spectrum is typical of proteins containing the canonical β-sheet conformation [21], the lack of which characterizes the CD spectrum of

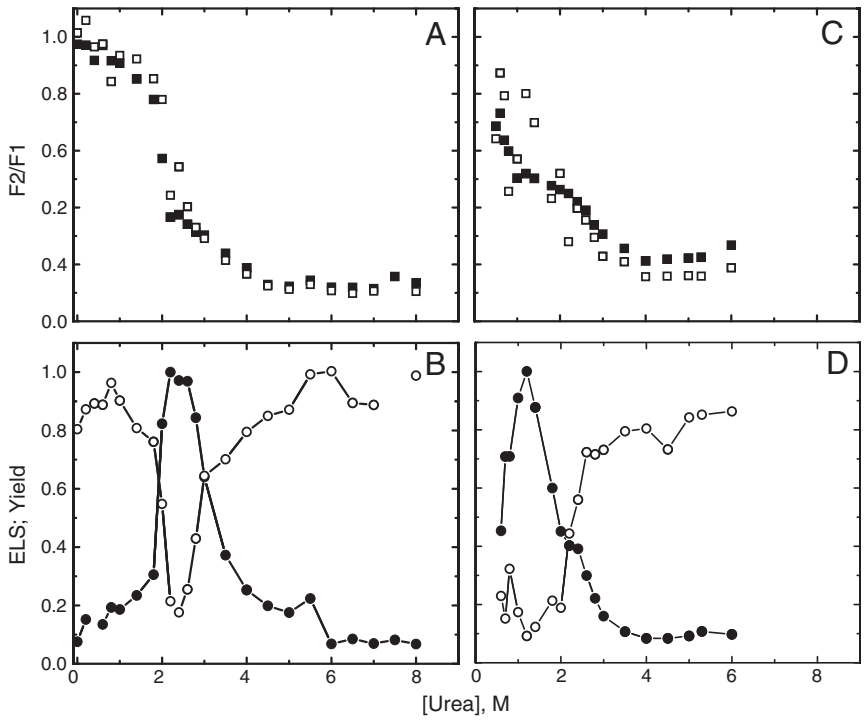

Fig. 4. The changes in the tertiary structure content and aggregation of MfpA induced by urea as monitored by changes in the position of fluorescence λ_{max}, fluorescence intensity and light scattering. The native (in buffer) or denatured (in 6.5 M urea) protein was incubated in the buffer with corresponding concentration of urea for 24 h after which the fluorescence spectra and light scattering (ELS) were measured. The samples were then centrifuged, the supernatants collected and the soluble protein yield (as the area under the fluorescence spectrum), the ratio of the fluorescence intensities F1/F2 and ELS of the supernatants were measured again immediately. Buffer: 25 mM Tris–HCl, 25 mM KCl, 4 mM $MgCl_2$, 0.1 mM EDTA, 6% Glycerol, 2 mM DTT, pH 7.6. A, B – The denaturation of MfpA by urea; C, D – Refolding of MfpA from 6.5 M urea; A, C – filled symbols represent the data obtained before centrifugation, open symbols – the data is taken after centrifugation; B, D: filled symbols represent the ELS data obtained before centrifugation, open symbols represent the protein left in the supernatant after centrifugation as monitored by fluorescence (yield).

the native MfpA (Fig. 3B and [6]). Its protein concentration independence suggests that the MfpA far-UV CD spectrum reports intramolecular rather than intermolecular changes. In contrast, the near-UV CD spectrum of MfpA completely disappears upon urea induced denaturation. Native secondary and tertiary structures are not recovered upon refolding (Fig. 3C). Refolding followed by the F1/F2 ratio (Fig. 4C) is characterized by a plateau in the fluorescence centered on the aggregation maximum (Fig. 4D).

3.3. Removal of aggregate by centrifugation

We hypothesized that the chemical denaturant, urea denatures MfpA through two stages. Urea first denatures MfpA through the structural states observed for thermal denaturation; native molecules, intermediates and MfpA aggregates are together in solution. Second, aggregate formed in the first stage dissociate and MfpA monomers are completely denatured at high urea concentration. If the exchange rates between these species are slow, removal of the aggregate would allow the properties of the soluble protein fraction (native, intermediate and completely denatured protein in different ratios) to be interrogated. We tested this hypothesis by ultracentrifuging urea containing solutions to remove aggregate. The yield of soluble protein was inversely related to the aggregate fraction reported by ELS consistent with our hypothesis (Fig. 4B, compare open & closed symbols).

The urea titration monitored by the F1/F2 ratio is unchanged following centrifugation (Fig. 4A). Since the F1/F2 ratio tracks the shift from native to the intermediate and denatured species, this constancy indicates that the intermediate structure is transformed before aggregation. Refolding of the soluble fraction tracked by the F1/F2 ratio is also unchanged by centrifugation (Fig. 4C). The plateau of the F1/F2 ratio coincident with the ELS peak (Fig. 4C & D) confirms formation of the intermediate structure preceding aggregation. The ELS signal reveals aggregates that are stable and remain in solution when urea is completely removed following refolding (Fig. 4D).

In summary, the urea denaturation and refolding studies together with the analysis of the soluble fraction following centrifugation are consistent with the model that rationalizes thermal denaturation and refolding; Dimer dissociation is followed by the monomers that in turn undergo a structural transition that predisposes them to aggregation. However, unlike the aggregate formed at high temperature, the aggregate formed at moderate concentrations of urea is not stable at high urea concentration. That there is also an energetic barrier that prevents dissociation of the urea denatured protein is shown by the residual aggregate present after refolding. The structural similarity between the thermal and chemically generated aggregate is reflected in the similarity of their CD spectra (Figs. 2 & 3).

3.4. Sodium dodecyl sulfate (SDS) denaturation and refolding of MfpA

The denaturation of proteins by detergents differs from the process induced by thermal and chemical denaturation. Ionic detergents can denature proteins at millimolar concentrations. They typically dissociate oligomers before denaturing monomers which may retain significant structure [25–28]. We have used the detergent SDS to stabilize the intermediate in MfpA denaturation to enable its characterization.

MfpA migrates as a single band corresponding to the protein monomer upon SDS-PAGE demonstrating that the detergent induces dissociation without aggregation (data not shown). MfpA's far-UV CD spectrum in SDS displays peaks that coincide with those of MfpA refolded from urea (Figs. 3B & 5A). The two negative peaks at

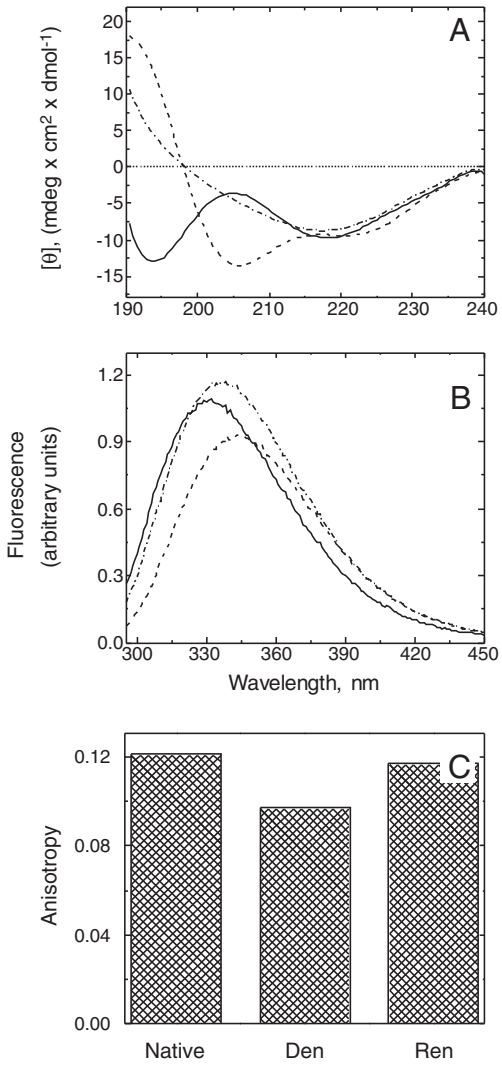

Fig. 5. A) Far-UV CD spectra, B) fluorescence spectra and C) change of the fluorescence anisotropy of MfpA as a function of the presence of SDS. Spectra for native, denatured and refolded MfpA are shown as solid, dashed and dot-dashed lines respectively. The protein concentration was 1 and 4 μM for the fluorescence and CD measurements respectively. Buffer: 5 mM Tris–HCl, 5 mM KCl and 2 mM DTT, pH 7.6.

~206 nm and 222 nm are characteristic of proteins in SDS [26,27], that typical of α/β proteins [21] and completely different from that of the native MfpA [4,6]. The fluorescence emission λ_{max} red shifts to ~342 nm indicating increased exposure of the Trp residues, again recapitulating urea refolded MfpA (Fig. 5B). However the magnitude of the decreases in fluorescence intensity (Fig. 5B) and anisotropy (Fig. 5C) of the SDS denatured MfpA indicate greater Trp solvent exposure than the urea denatured protein. This difference can be attributed to the small fluorescence change that occurs when the intermediates aggregate when refolded from urea.

These data show that the MfpA monomer in SDS has high secondary and tertiary structure content similar to that observed in urea refolded MfpA aggregate. The SDS titration mid-point is ~0.5 mM corresponding to 4–5 detergent molecules bound to each MfpA monomer (Fig. 6). When SDS denaturation occurs at concentrations below the critical micelle concentration, protein oligomer dissociation rather than subunit denaturation is typically observed [26,29]. The relatively small numbers of SDS molecules that bind to MfpA as well as the changes in the spectral measures are consistent with this view. In SDS, the MfpA dimer dissociates to monomers. These monomers transform to an intermediate conformation, similar to that observed upon thermal and chemical denaturation, but are prevented from aggregating by the detergent.

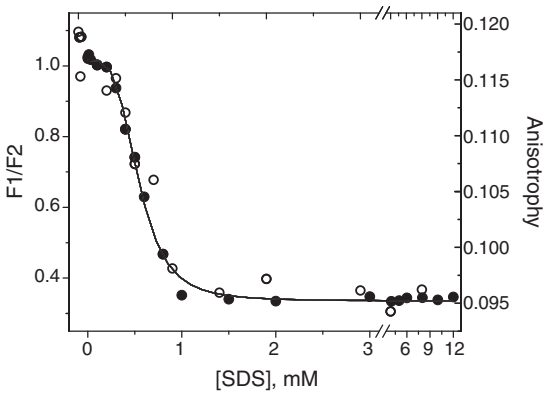

Fig. 6. Shift of the fluorescence spectra (filled circles) and anisotropy (open circles) as a function of the SDS concentration. F1/F2 – ratio of fluorescence intensities at the wings of the fluorescence spectrum. Buffer: 5 mM Tris–HCl, 5 mM KCl and 2 mM DTT, pH 7.6.

4. Discussion

4.1. Biological significance of protein misfolding and aggregation

The view that protein misfolding followed by aggregation is an *in vitro* artifact dissipated with the discovery and understanding of protein misfolding diseases (amyloidoses) such as Alzheimer's, Parkinson's, prion-linked diseases and cataracts [7], inclusion bodies formation when proteins are over expressed in bacteria [8] and drug storage and delivery [30]. Protein misfolding and aggregation are part of the natural folding energy landscape [31] and may be initiated through thermal fluctuations occurring under physiological conditions [11]. Functional amyloid fibers have been identified in bacteria, fungi, insects, invertebrates and humans [32]. The discovery of functional amyloid in *E. coli*[33] and gram-positive bacteria [34] provides incentive for further study of this phenomenon in highly pathogenic bacteria such as *M. tuberculosis*.

4.2. Energetics of MfpA denaturation and refolding

Poor thermal and environmental stability limit the application of thermodynamic analysis to protein structural and unfolding reactions that are not freely reversible. Thermodynamic functions, such as changes in entropy and Gibbs functions [9,10] can not be extracted from temperature-induced irreversible denaturation reactions. However in many cases protein irreversible denaturation can be described by kinetic models such as that of Lumry–Eyring [15,35]. The Lumry–Eyring model postulates that a denaturation process can be modeled as a rapid equilibrium between the native structure and an intermediate ($N \leftrightarrow I$) that is followed by a rate limiting conversion of the intermediate to the final denatured state ($I \rightarrow F$). Evidence supporting application of this model is the existence of the "kinetic trap" shown earlier for MfpA denaturation [6]. We therefore applied the Lumry–Eyring model to the temperature denaturation transitions of MfpA (see Supplementary Material for details).

The transition mid-points for the multiple measures of structural changes used to follow the temperature-induced denaturation and refolding reactions are almost coincident except for fluorescence $\Delta\lambda_{max}$ (Figs. 2 & 1S, Table 1). The F1/F2 ratio that quantitatively tracks $\Delta\lambda_{max}$[14] and $\Delta\lambda_{½}$ values measured at high temperature reflect high polarity and a homogeneous environment surrounding MfpA's three tryptophan residues. Of these three residues, the only buried tryptophan (W154) is located at the dimer interface (Fig. 7C). The observation that F1/F2 transitions at a lower temperature than the

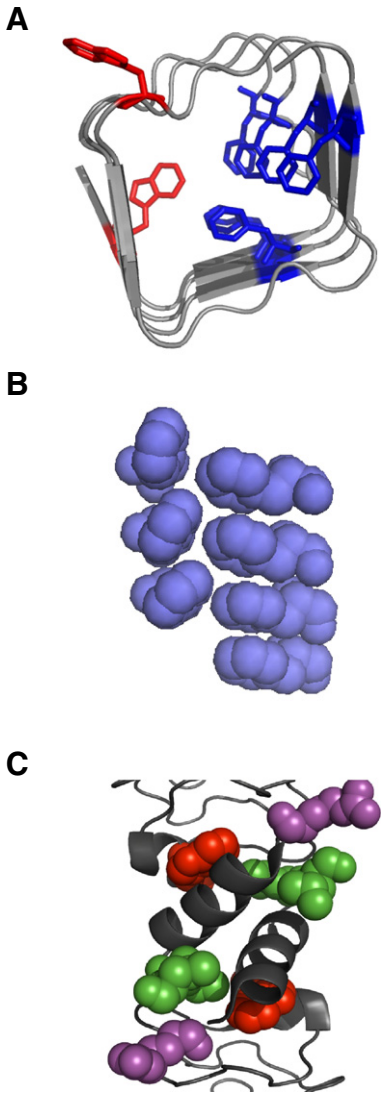

Fig. 7. Distribution of phenylalanine residues within the N-terminus of MfpA with (A) or without (B) the backbone of the PRP motif; (C) Distribution of the Trp, Leu and Arg residues along with the α – helices inside C-terminus of MfpA at the dimer interface; Blue – Phe, Red –tryptophan; Green – Leu; Magenta – Arg.

parameters that track global structure and aggregation indicates that dimer dissociation precedes the structural transformation of monomers that in turn leads to aggregation (Table 1). This transformation is not reversible because of the high Arrhenius activation energy for aggregation (Fig. 2, open symbols; Table 1). This conclusion was validated by the urea denaturation studies.

Three possibilities are considered: i) if a protein aggregates most strongly under native conditions, then the main species that aggregates will be native in structure; ii) if denatured protein preferentially aggregates, then the main species that aggregates is denatured in structure; iii) if aggregation is strongest under conditions that are intermediate between native and denatured, then the aggregating species is an intermediate conformation. The maximal aggregation measured at the mid-points of the denaturation and refolding transitions clearly favors scenario iii (Fig. 4).

We next asked whether the structural changes precede or follow aggregation. Since all detectable secondary and tertiary structure is lost at high urea concentrations the nature of the 'denatured' ensemble does not appear to dictate the structure of refolded MfpA (Fig. 4). The concentration independence of the secondary structure changes measured for MfpA refolding is consistence with intramolecular rather than intermolecular interactions (Fig. 3B). Lastly, the lack of concordance of the changes in the F1/F2 ratio and aggregation upon refolding indicates that the structure of the intermediates does not change upon aggregation (Fig. 4C & D). This multiple lines of evidence provide compelling evidence in support scenario *iii* and points to aggregation of the intermediate rather than denatured MfpA conformation.

The SDS titration mid-point of ~0.5 mM is below the 3–5 mM critical micelle concentration [29,36] and corresponds to 4–5 detergent molecules bound to each MfpA monomer (Fig. 6). At sub-micellular concentrations SDS typically does not influence protein structure [26]. It preferentially binds to cationic groups on the protein that are located around hydrophobic clefts within which the surfactant side chain can be accommodated [37]. The dimer interface of MfpA fits well these criteria for SDS binding. The hydrophobic pocket of the dimer interface is formed by two Trp, four Leu and the hydrophobic side chains of two α- helices framed by two Arg residues (Fig. 7C). The anionic group of the SDS molecule is envisioned to binds to the cationic group of the Arg residues thus placing the alkyl chain of SDS in the hydrophobic pocket of the dimer interface (Fig. 7C). That MfpA's only α-helices are located in this pocket make the dimer interface the probable binding site for SDS [38].

The spectral data suggests that dissociated MfpA monomers are unstable and rapidly transform into the intermediate conformation. Although contemporary calculation methods poorly capture the secondary structure content of α/β proteins [39], the shape of the far-UV CD spectra of the SDS denatured MfpA is typically for α/β [21] and completely different from that of native MfpA (Fig. 5A). Bound SDS prevents formation of the aggregate observed in thermally and chemically denatured MfpA; β-sheet proteins are stable in SDS containing solution [38]. Further support for SDS denatured MfpA having the same or similar structure as the aggregation prone intermediate in thermal and chemical denaturation is the correspondence of the CD spectra of MfpA aggregate refolded from urea with that of the MfpA monomers in SDS (Fig. 3 & 5). Clearly dimerization plays a critical role in stabilizing the pentapeptide fold of MfpA.

4.3. The energetic landscape of MfpA denaturation and refolding

Protein folding can follow multiple pathways to the final native structure. Since there is no a single route to the native state, our view

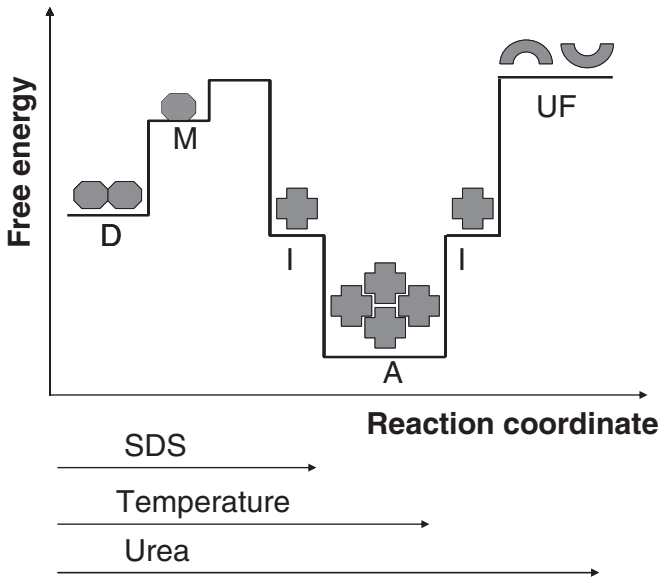

Fig. 8. An energy diagram of the MfpA structural transitions and accompanying aggregation induced by temperature, urea and SDS. M – monomer, D – dimer, I – intermediate, A – aggregate, UF – unfolded.

of folding has evolved to that of a 'landscape' in which the unfolded polypeptide chain searches for the native conformation along an energy surface until the unique native structure is formed [33]. The denaturation and refolding of MfpA can be described by the 'double funnel' energy landscape [40] where the 'native' and 'aggregation' funnels are separated by a high kinetic energy barrier that is not overcome during equilibrium refolding *in vitro*. Fig. 8 shows a simplified two-dimensional scheme to represent the landscape that rationalizes the denaturation and refolding of MfpA induced by the multiple denaturants studied.

The presence of a high energy barrier but not a difference in the energy of native and intermediate forms of MfpA defines the probability of the structural transition. During denaturation, the MfpA dimer first dissociates. The native-like monomers then undergo a structural transition making them prone to aggregate. The aggregate does not precipitate; they are in equilibrium with the transformed monomeric intermediates. Dissociation of the aggregate and complete denaturation of the monomers occurs at high detergent concentration. The structure of intermediates contains the typical β-sheet conformation absent in the PRP fold of the native MfpA (Fig. 3B and [6]) and lacks the stabilizing stacking interactions characteristic for the native PRP fold (see below). The intermediate structure is the same in the monomeric or aggregate states. The highest energy barrier is between the aggregates and the native protein.

4.4. DNA mimicry by MfpA; phenylalanine side chain stacking stabilizes the N-terminus of MfpA

Documented DNA mimicry by proteins typically includes the negative charge of the phosphate backbone, hydrogen-bonding properties of the nucleotide bases and the bending and twisting of the DNA double helix [2]. Native, but not temperature/urea denatured or refolded MfpA, has a distinctive near-UV CD spectrum (Fig. 1 & 3) resulting from strong coupling of the aromatic transitions [20]. Seven of the ten phenylalanine residues and two of the three tryptophan residues reside in the N-terminus of MfpA (Fig. 7). The coils of the pentapeptide repeat fold stack directly atop one another [4] with the phenylalanine side chains forming two stacks inside the tube formed by the first four complete coils (Fig. 7).

The stacks appear to stabilize the PRP fold analogously to nucleotide base-pair stacking inside double-helical DNA. Denatured and refolded MfpA lack this defining characteristic of the native protein. Stabilization by phenylalanine side chain stacking of the N-terminal portion of MfpA's pentapeptide repeat expands the motif of DNA mimicry beyond size, shape and surface charge. These stacking interactions together with interaction of the MfpA monomer C-termini upon dimerization are crucial characteristics that stabilize the native PRP fold of MfpA.

Acknowledgment

This study was supported by grant R01GM079618 from the National Institutes of Health.

Appendix A. Supplementary data

Supplementary data to this article can be found online at doi:10.1016/j.bpc.2011.04.015.

References

[1] S. Hegde, M. Vetting, S. Roderick, L. Mitchenall, A. Maxwell, H. Takiff, S. Blanchard, A fluoroquinolone resistance protein from *Mycobacterium tuberculosis* that mimics DNA, Science 308 (2005) 1480–1483.
[2] D. Dryden, M. Tock, DNA mimicry by proteins, Biochem. Soc. Trans. 34 (2006) 317–319.
[3] A. Maxwell, Gyrase as a drug target, Trends Microbiol. 5 (1997) 102–109.
[4] M. Vetting, S. Hegde, J. Fajaro, A. Fiser, S. Roderick, H. Takiff, S. Blanchard, Pentapeptide repeat proteins, Biochemistry 45 (2006) 1–10.
[5] J.C. Wang, Cellular roles of DNA topoisomerases: a molecular perspective, Nat. Rev. Mol. Cell Biol. 3 (2002).
[6] S. Khrapunov, H. Cheng, S. Hegde, J. Blanchard, M. Brenowitz, Solution structure and refolding of the *Mycobacterium tuberculosis* pentapeptide repeat protein MfpA, J. Biol. Chem. 283 (2008) 36290–36299.
[7] F. Chiti, C. Dobson, Protein misfolding, functional amiloid, and human disease, Annu. Rev. Biochem. 75 (2006) 333–366.
[8] G. Georgiu, P. Valax, Isolation inclusion bodies from bacteria, Methods Enzymol. 309 (1999) 48–58.
[9] C.N. Pace, Determination and analysis of urea and guanidine hydrochloride denaturation curves, Methods Enzymol. 13 (1986) 266–280.
[10] P.L. Privalov, Thermodynamic problems of protein structure, Annu. Rev. Biophys. Biophys. Chem. 18 (1989) 47–69.
[11] D. Shortle, M. Ackerman, Persistence of native-like topology in a denatured protein in 8 M urea, Science 293 (2001) 487–489.
[12] O. Ptytsyn, Molten globule and protein folding, Adv. Protein Chem. 47 (1995) 83–229.
[13] K. Vassilenko, V. Uversky, Native-like secondary structure of molten globules, Biochim. Biophys. Acta 1594 (2002) 168–177.
[14] S.N. Khrapunov, A.I. Dragan, A.V. Sivolob, A.M. Zagariya, Mechanisms of stabilizing nucleosome structure. Study of dissociation of histone octamer from DNA, Biochim. Biophys. Acta 1351 (1997) 213–222.
[15] J.M. Sanchez-Ruiz, Theoretical analysis of Lumry–Eyring models in differential scanning calorimetry, Biophys. J. 61 (1992) 921–935.
[16] M.R. Eftink, The use of fluorescence methods to monitor unfolding transitions in proteins, Biophys. J. 66 (1994) 482–501.
[17] J.R. Lakowicz, Principles of fluorescence spectroscopy, 2 ed. Kluwer Academic/Plenum, New York, 1999.
[18] R. Renthal, An unfolding story of helical transmembrane proteins, Biochemistry 45 (2006) 14559–14566.
[19] S.Y. Venyaminov, J.T. Yang, Determination of protein secondary structure, in: G.D. Fasman (Ed.), Circular dichroism and the conformational analysis of biomolecules, Plenum Press, New York, 1996, pp. 69–107.
[20] N. Sreerama, M.C. Manning, M.E. Powers, J.X. Zhang, D.P. Goldenberg, R.W. Woody, Tyrosine, phenylalanine, and disulfide contributions to the circular dichroism of proteins: circular dichroism spectra of wild-type and mutant bovine pancreatic trypsin inhibitor, Biochemistry 38 (1999) 10814–10822.
[21] N. Sreerama, R. Woody, Computation and analysis of protein circular dichroism spectra, Methods Enzymol. 383 (2004) 318–351.
[22] S.M. Kelly, T.J. Jess, N.C. Price, Title: how to study proteins by circular dichroism, Biochim. Biophys. Acta 1751 (2005) 119–139.
[23] C.N. Pace, K.L. Shaw, Linear extrapolation method of analyzing solvent denaturation curves, Proteins 4 (2000) 1–7.
[24] M.M. Santoro, D.W. Bolen, Unfolding free energy changes determined by the linear extrapolation method. 1. Unfolding of phenylmethanesulfonyl alpha-chymotrypsin using different denaturants, Biochemistry 27 (1988) 8063–8068.
[25] F. Lau, J. Bowie, A method for assessing the stability of a membrane protein, Biochemistry 36 (1997) 5884–5892.
[26] H.L. Bagger, S.V. Hoffmann, C.C. Fuglsang, P. Westh, Glycoprotein-surfactant interactions: a calorimetric and spectroscopic investigation of the phytase-SDS system, Biophys. Chem. 129 (2007) 251–258.
[27] L. Visseri, E.R. Bloutj, Elastase. 11. Optical properties and the effects of sodium dodecyl sulfate, Biochemistry 10 (1971) 743–752.
[28] F.W. Lau, J.U. Bowie, A method for assessing the stability of a membrane protein, Biochemistry 36 (1997) 5884–5892.
[29] B. Maestro, J.M. Sanz, Extensive unfolding of the C-LytA choline-binding module by submicellar concentrations of sodium dodecyl sulphate, FEBS Lett. 581 (2007) 375–381.
[30] I. Kim, W. Xu, J.C. Reed, Cell death and endoplasmic reticulum stress: disease relevance and therapeutic opportunities, Nat. Rev. Mol. Cell Biol. 7 (2008) 1013–1030.
[31] P.G. Wolynes, Energy landscapes and solved protein-folding problems, Philos. Trans. R. Soc. Lond. A 363 (2005) 453–467.
[32] D. Fowler, A. Koulov, W. Balch, J.W. Kell, Functional amyloid – from bacteria to humans, Trends Biochem. Sci. 32 (2007) 217–224.
[33] M. Chapman, L. Robinson, J. Pinkner, R. Roth, J. Heuser, M. Hammar, S. Normark, S. Hultgren, Role of *Escherichia coli* curli operons in directing amyloid fiber formation, Science 295 (2002) 851–855.
[34] P.B. Jordal, M.S. Dueholm, P. Larsen, S.V. Petersen, J.J. Enghild, G. Christiansen, P. Højrup, P.H. Nielsen, D.E. Otzen, Widespread abundance of functional bacterial amyloid in mycolata and other gram-positive bacteria, Appl. Environ. Microbiol. 75 (2009) 4101–4110.
[35] R. Lumry, H. Eyring, Conformation changes of proteins, J. Phys. Chem. 58 (1954) 110–120.
[36] P. Sehgal, J.E. Mogensen, D.E. Otzen, Using micellar mole fractions to assess membrane protein stability in mixed micelles, Biochim. Biophys. Acta 1716 (2005) 59–68.
[37] M.R. Housaindokht, A.A. Moosavi-Movahedi, J. Moghadasi, M.N. Jones, Interaction of glucose oxidase with ionic surfactants: a microcalorimetric study, Int. J. Biol. Macromol. 15 (1993) 337–341.
[38] M.M. Nielsen, K.K. Andersen, P. Westh, D. Otzen, Unfolding of β-sheet proteins in SDS, Biophys. J. 92 (2007) 3674–3685.
[39] S. Khrapunov, Circular dichroism spectroscopy has intrinsic limitations for protein secondary structure analysis, Anal. Biochem. 389 (2009) 174–176.
[40] P.L. Clark, Protein folding in the cell: reshaping the folding funnel, Trends Biochem. Sci. 29 (2004) 527–534.